Dark cores in sunspot penumbral filaments

Göran B. Scharmer, Boris V. Gudiksen, Dan Kiselman, Mats G. Löfdahl & Luc H. M. Rouppe van der Voort

The Institute for Solar Physics of the Royal Swedish Academy of Sciences, AlbaNova University Centre, SE-106 91 Stockholm, Sweden

Sunspot umbrae—the dark central regions of the spots—are surrounded by brighter filamentary penumbrae, the existence of which remains largely inexplicable[1]. The penumbral filaments contain magnetic fields with varying inclinations[2] and are associated with flowing gas[3–5], but discriminating between theoretical models[6–8] has been difficult because the structure of the filaments has not hitherto been resolved. Here we report observations of penumbral filaments that reveal dark cores inside them. We cannot determine the nature of these dark cores, but their very existence provides a crucial test for any model of penumbrae. Our images also reveal other very small structures, in line with the view that many of the fundamental physical processes in the solar photosphere occur on scales smaller than 100 km.

The best spatial resolution attained in solar observations has typically been about 0.2 arcsec (150 km). The Swedish 1-m Solar Telescope[9] at the Roque de los Muchachos on the Canary island of La Palma is a newly installed (spring 2002), evacuated refractor designed to significantly improve this. The main obstacle to diffraction-limited imaging is rapidly varying aberrations from temperature inhomogeneities in the Earth's atmosphere. These effects, referred to as 'seeing', are corrected for by low-order adaptive optics (15 corrected modes), real-time frame selection (picking the best images from a continuous stream of exposures), and subsequent image restoration using a variant[10] of the phase-diversity technique[11,12]. The resolution achieved is better than 0.12 arcsec.

A notable feature in our best images of sunspots is that many penumbral filaments, which are isolated from the bulk of the penumbra and surrounded by dark umbra, show dark cores. The footpoints of the dark cores appear mostly adjacent to—and in some cases, centred on—peripheral umbral dots (small bright features standing out near the edge of the dark umbra) or penumbral grains (brighter parts of penumbral filaments that move radially). These footpoints are in constant motion, sometimes appearing to pass in front of (above), or splitting, the bright dot or grain. Branching of the dark core into several cores can sometimes be seen close to a footpoint (Figs 1 and 2d). The widths of the filaments close to their point of origin are consistently 150–180 km (5–6 image pixels), as measured between the intensity maxima on either side of the dark core on filaments isolated enough to show such maxima. We propose this to be a typical dimension of the structure. The dark cores are unresolved, and could be much narrower than their measured full-width at half-minimum of 90 km. They can be very long compared to their width, and some can be followed for more than 1,000 km (Figs 1, 2 and 3d). The dark-cored filaments can be symmetric (Fig. 2a, d, e), slightly asymmetric (Fig. 2b) or strongly (Fig. 2c) asymmetric.

Deformation of images by 'seeing' can in principle produce spurious double structures. We are, however, confident that the dark cores shown here are real. They look qualitatively the same at the different wavelength bands we have used (430.5 nm, 436.4 nm, 487.7 nm), phase-diversity restored images show them, and they persist over many frames in our best data (see movie in Supplementary Information).

Not all isolated filaments show the dark-core structures but they are found in all spots for which we have excellent data covering at least several minutes. The lifetimes of the dark cores are similar to the lifetimes of the filaments themselves; they can last for at least one hour.

An interesting variety of dark-cored filaments are the fainter structures in the umbra, of which Fig. 2e shows an example. These features are associated with the inward migration of a bright dot followed by repeated brightening and fading on a timescale of minutes. This suggests that a larger fraction of umbrae than observed so far could have faint or small-scale filamentary structure[13].

The description above applies to spots close to the centre of the solar disk and thus with a nearly vertical line of sight. We have not found clear and symmetric dark-cored filaments in spots closer to the limb. This could be due to their three-dimensional structure and the oblique viewing angle.

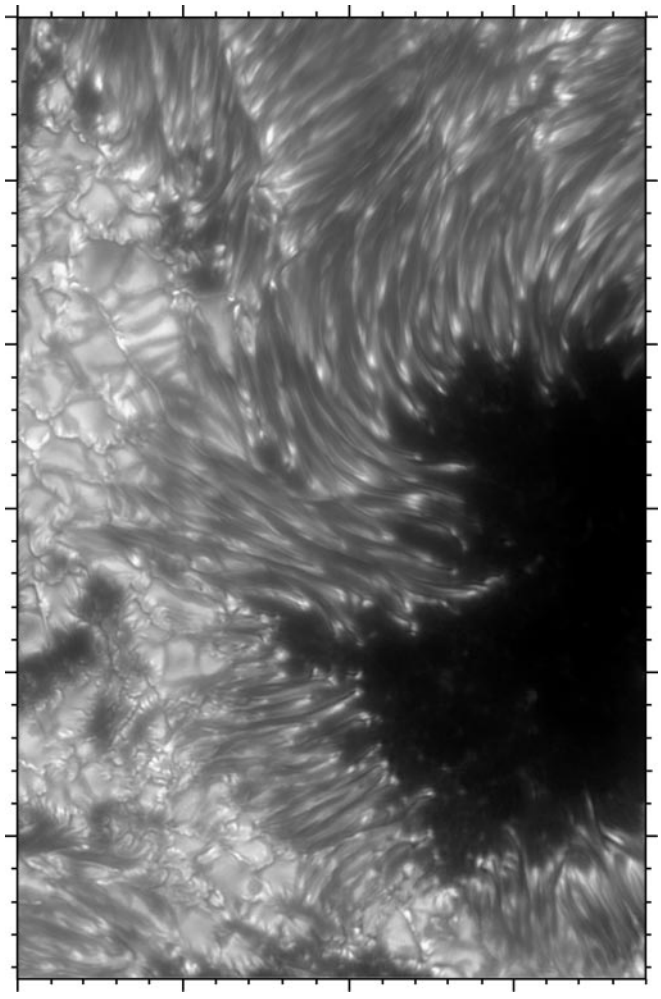

Figure 1 Part of the largest spot in active region 10030 on 15 July 2002 recorded with the Swedish 1-m Solar Telescope using adaptive optics (as are all images shown here). The telescope has an unobstructed aperture of 96 cm and a focal length of 20.3 m at 460 nm wavelength which gives an image scale of 0.041 arcseconds per pixel. The chromatic aberrations from the singlet objective, acting also as vacuum window, are nearly perfectly compensated by an in-vacuum Schupmann corrector. This image was phase-diversity restored, and to that end the camera was equipped with a beamsplitter that puts two images on the same charge-coupled device (CCD) with a known defocus for one of the images. A narrow-band filter centred on 430.5 nm was used. The exposure time was 6 ms. Tickmarks have a spacing of 1,000 km on the Sun. About half of the dark umbra of the sunspot is seen to the right, the surrounding granulation to the left with penumbral structures in between. Many penumbral filaments with dark cores are seen protruding into the umbra, notably in the mass of filaments in the centre of the image. The spectral band used is at the location of the G-band spectral feature (formed by spectral lines of the CH radical), but it should be noted that the dark cores show up also in continuum bands.

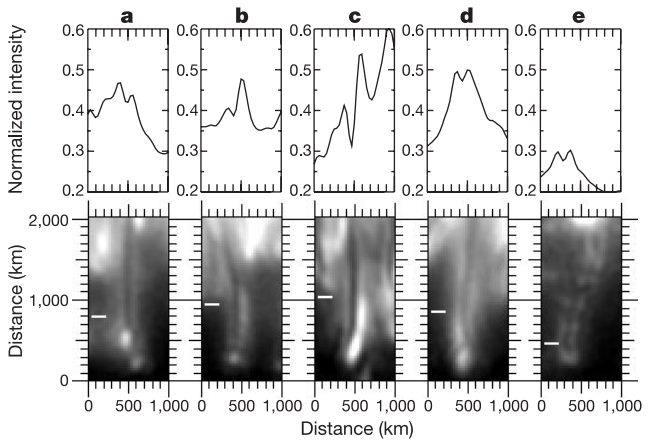

Figure 2 Examples of penumbral filaments with dark cores. Plots (top row) show intensity profiles at indicated sections of the images (bottom row). Intensity values are given in units of the surrounding photosphere from the same exposures. Spatial tickmarks have 100-km spacing. From the largest spot of active region 9957 on 22 May 2002: **a**, G-band (3.3 ms), **b**, G-band (3.3 ms). From the largest spot of active region 10030 on 15 July 2002: **c**, G-band (6 ms). **d**, 487.7-nm continuum (13 ms). **e**, 487.7-nm continuum (13 ms). **a**, **b**, **d** and **e** are corrected for the modulation transfer function (MTF) of the diffraction-limited telescope and the detector by Wiener filtering. Panel **c** is phase-diversity restored, and is thus filtered using a measured optical transfer function.

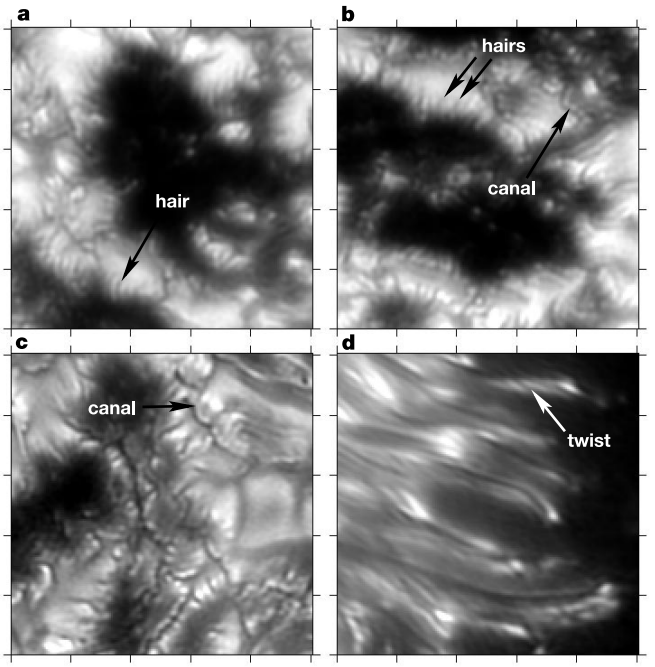

Figure 3 Thin dark features in active region 10030 on 15 July 2002. **a**–**c**, Pores with hair-like features around their edges and 'canals' in their surroundings. The 'canals' look like more stable and narrow versions of intergranular lanes. **d**, Dark-cored filaments and a filament with dark streaks making it look twisted. Panels **a** and **b** are MTF-filtered 487.7-nm continuum (13 ms); **c** and **d** are phase-diversity restored G-band (6 ms). Tickmarks have 1,000 km spacing.

The data we have obtained so far do not give direct information on fluid velocities or magnetic fields (additional instrumentation is required for this), and thus any interpretation of the dark-cored filaments must be speculative. They could be caused by two (or more) thin bright filaments that happen to pair up in parallel. The consistent separation of these filaments, as well as the very stable behaviour of the dark cores when seen in movies (Supplementary Information), make this explanation unlikely. Such thin (<100 km) and long (>1,000 km) bright filaments would put strong constraints on the mechanisms supplying them with energy without which they would rapidly cool and become invisible[14].

A dark-cored filament could be produced by an optically thin cylindrical tube with hot walls—perhaps a magnetic flux tube heated on the surface by the dissipation of electrical currents. Estimates show, however, that the currents induced by a twist of the tube[15] are insufficient, and topological dissipation[16] (from movements of the flux-tube footpoints) can hardly explain why so few individual flux tubes would be subjected to excess heating for so long.

Inspection of our images shows numerous varieties of other very thin dark lines in magnetic regions that are exemplified in Fig. 3: 'hairs' that are seemingly emanating from pores into the closest neighbouring granules, 'canals' in the granulation near spots and pores, and running dark streaks crossing penumbral filaments diagonally. (These streaks make the filaments look as if they are twisting with minute-long periods and several turns along their length.) Frequently these structures give a visual impression of something dark and opaque lying on top of brighter structures. However, we are cautious about subjective image interpretations. An argument against such top-heavy configurations is that they would be prone to Rayleigh–Taylor instability[17].

Although the sophistication of, and computational resources for, numerical modelling and simulations of complex radiative hydrodynamics and magnetohydrodynamics in the solar atmosphere have improved at an impressive rate during the last decade, it has become increasingly clear that further progress needs observations at higher spatial resolution than is so far achievable. We believe that the observations presented here represent a significant improvement in spatial resolution, while also indicating that fundamental physical scales of solar processes are finally becoming observable. □

Received 19 August; accepted 1 October 2002; doi:10.1038/nature01173.

1. Parker, E. *Sunspots: Theory and Observations* (eds Thomas, J. H. & Weiss, N. O.) 413–423 (Kluwer, Dordrecht, 1992).
2. Title, A. *et al.* On the magnetic and velocity field geometry of a simple sunspot. *Astrophys. J.* **403,** 780–796 (1993).
3. Evershed, J. Radial movement in sun-spots. *Mon. Not. R. Astron. Soc.* **69,** 454–457 (1909).
4. Muller, R. Étude morphologique et cinématique des structures fines d'une tache solaire. *Sol. Phys.* **29,** 55–73 (1973).
5. Sobotka, M., Brandt, P. N. & Simon, G. W. Fine structure in sunspots. III. Penumbral grains. *Astron. Astrophys.* **348,** 621–626 (1999).
6. Danielson, R. E. The structure of sunspot penumbras. II. Theoretical. *Astrophys. J.* **134,** 289–311 (1961).
7. Montesinos, B. & Thomas, J. H. The Evershed effect in sunspots as a siphon flow along a magnetic flux tube. *Nature* **390,** 485–487 (1997).
8. Schlichenmaier, R., Jahn, K. & Schmidt, H. U. Magnetic flux tubes evolving in sunspots. A model for the penumbral fine structure and the Evershed flow. *Astron. Astrophys.* **337,** 897–910 (1998).
9. Scharmer, G. B., Bjelksjö, K., Korhonen, T. K., Lindberg, B. & Pettersson, B. *Innovative Telescopes and Instrumentation for Solar Astrophysics* (eds Keil, S. & Avakyan, S.) Vol. 4853-47 *Proc. SPIE* (in the press).
10. Löfdahl, M. G. *Image Reconstructions from Incomplete Data II* (eds Bones, P. J., Fiddy, M. A. & Millanc, R. P.) Vol. 4792-21 *Proc. SPIE* (in the press).
11. Löfdahl, M. G., Berger, T. E. & Seldin, J. H. Two dual-wavelength sequences of high-resolution solar photospheric images captured over several hours and restored by use of phase diversity. *Astron. Astrophys.* **377,** 1128–1135 (2001).
12. Thomas, J. H. Solar physics: The sun at small scales. *Nature* **396,** 114–115 (1998).
13. Livingston, W. Radial filamentary structure in a sunspot umbra. *Nature* **350,** 45–46 (1991).
14. Schlichenmaier, R., Bruls, J. H. M. J. & Schüssler, M. Cooling of a hot flux tube in the solar photosphere. *Astron. Astrophys.* **349,** 961–973 (1999).
15. Galsgaard, K. & Nordlund, Å. Heating and activity of the solar corona. 2. Kink instability in a flux tube. *J. Geophys. Res.* **102,** 219–230 (1997).
16. Parker, E. N. Topological dissipation and the small-scale fields in turbulent gases. *Astrophys. J.* **174,** 499–510 (1972).
17. Spruit, H. C. *The Role of Fine-scale Magnetic Fields on the Structure of the Solar Atmosphere* (eds Schröter, E. H., Vazquez, M. & Wyller, A. A.) 199–209, (Cambridge Univ. Press, Cambridge, 1987).

Supplementary Information accompanies the paper on *Nature*'s website (http://www.nature.com/nature).

Acknowledgements The Swedish 1-m Solar Telescope is operated on the island of La Palma by the Royal Swedish Academy of Sciences in the Spanish Observatorio del Roque de los Muchachos of the Instituto de Astrofisica de Canarias.

Competing interests statement The authors declare that they have no competing financial interests.

Correspondence and requests for materials should be addressed to D.K. (e-mail: dan@astro.su.se).

High-power terahertz radiation from relativistic electrons

G. L. Carr*, Michael C. Martin†, Wayne R. McKinney†, K. Jordan‡, George R. Neil‡ & G. P. Williams‡

** National Synchrotron Light Source, Brookhaven National Laboratory, Upton, New York 11973, USA*
† Advanced Light Source Division, Lawrence Berkeley National Laboratory, Berkeley, California 94720, USA
‡ Free Electron Laser Facility, Jefferson Laboratory, 12000 Jefferson Avenue, Newport News, Virginia 23606, USA

Terahertz (THz) radiation, which lies in the far-infrared region, is at the interface of electronics and photonics. Narrow-band THz radiation can be produced by free-electron lasers[1] and fast diodes[2,3]. Broadband THz radiation can be produced by thermal sources and, more recently, by table-top laser-driven sources[4–6] and by short electron bunches in accelerators[7], but so far only with low power. Here we report calculations and measurements that confirm the production of high-power broadband THz radiation from subpicosecond electron bunches in an accelerator. The average power is nearly 20 watts, several orders of magnitude higher than any existing source, which could enable various new applications. In particular, many materials have distinct absorptive and dispersive properties in this spectral range, so that THz imaging could reveal interesting features. For example, it would be possible to image the distribution of specific proteins or water in tissue, or buried metal layers in semiconductors[8,9]; the present source would allow full-field, real-time capture of such images. High peak and average power THz sources are also critical in driving new nonlinear phenomena and for pump–probe studies of dynamical properties of materials[10,11].

The THz region (1 THz ≈ 33 cm^{-1} or 4 meV) lies in the far-infrared spectral range where conventional thermal sources are very weak. For example, a blackbody source at 2,000 K provides less than 1 μW per cm^{-1} of spectral power density for a typical spectroscopy application. Whereas narrowband sources have been available using free-electron laser (FEL) technology[1,12], a significant advance in broadband THz sources has occurred over the past decade with the advent of coherent THz radiation emission from photocarriers in biased semiconductors. Table-top systems using optical rectification of femtosecond lasers either at high repetition rates[5] or high peak power[6] are routinely available.

The present work describes a different process for producing coherent THz radiation by accelerated electrons. Like the method described in ref. 5, the process begins with pulsed laser excitation in GaAs, but makes use of photoemission to produce bunches of free electrons in space. Using the energy-recovered linac (ERL) at the Jefferson Laboratory FEL[13], very short electron bunches (~500 fs) are brought to relativistic energies (~40 MeV) in a linac and then transversely accelerated by a magnetic field to produce the desired THz emission as synchrotron radiation. This unique accelerator is capable of a running with a relatively high average beam current (up to 5 mA). Like the THz emitter described in ref. 5, the electrons experience a common acceleration. If the electron bunch dimensions are small (in particular, the bunch length is less than the wavelength of observation), we again obtain a multiparticle coherent enhancement[14,15]. Such coherent synchrotron radiation has been observed from electrons accelerated in linacs[7,16–18], from compact waveguide FELs[19] and from magnetic undulators[19–21]. Coherent THz radiation has been discussed, and observed from electron bunches in storage rings[22–25], but not yet stably enough for use as a light source. Active programmes to study THz radiation from linacs or storage rings are underway at BESSY II (Berliner Elektronenspeicherring-Gesellschaft für Synchrotronstrahlung; www.bessy.de) and DESY (Deutsches Elektronen Synchrotron) in Germany, and at Brookhaven National Laboratory and Lawrence Berkeley National Laboratory in the USA. In addition, programmes are underway at ENEA-Frascati to generate broadband THz radiation by exploiting the distinctive properties of waveguide FELs which arise when the electron velocity is close to the group velocity of the wave packet[26]. Some linacs can create very short bunches (<1 ps) and produce coherent radiation up to a few THz, but most are limited to repetition rates of a few Hz, so the average power is quite low. The repetition rate for storage rings is of the order of 100 MHz, but the electron bunches are significantly longer (~100 ps) owing to longitudinal damping through synchrotron radiation emission. Thus the emission is limited to the very low frequency regime (far-infrared), or arises from instabilities that briefly modify the bunch shape.

Our ERL accelerator system overcomes some of the limitations of conventional linacs and storage rings. Electron bunches as short as ~500 fs are produced by the standard technique of energy modulation (chirping) followed by compression in the dispersive region of a magnetic chicane[27]. The time taken for an electron bunch to pass through the accelerator is less than 1 μs; thus longitudinal damping is negligible. But unlike most linacs, our system operates at a very high repetition rate (up to 75 MHz) by using superconducting radio frequency cavities and recovering the energy of the spent electron bunches[13] so that the average current is orders of magnitude higher than in conventional linacs.

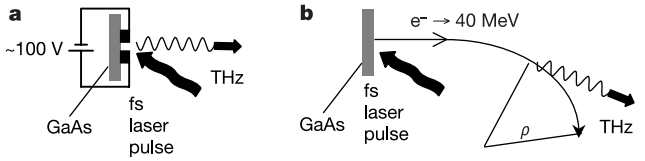

Figure 1 Comparison between coherent THz radiation generated by an 80-MHz conventional laser-driven THz source (**a**) and the relativistic source described here (**b**). In **a**, the photo-induced carriers immediately experience a force from the bias field (~100 V across a 100 μm gap) of ~10^6 V m^{-1}, which results in an acceleration of 10^{17} m s^{-2}. The entire process is completed in less than 1 ps, resulting in spectral content up to a few THz. In **b**, approximately the same number of charge carriers are brought to a relativistic energy of >10 MeV in a linac, after which a magnetic field bends their path into a circle of radius $\rho = 1$ m, resulting in an acceleration $c^2/\rho = 10^{17}$ m s^{-2}, the same as for **a**. An observer of **b** would also detect a brief pulse of electromagnetic radiation as an electron bunch passed by. But in this case, two factors control the pulse duration; one is the bunch length, and the other is the time for the relativistically compressed acceleration field from each electron to sweep past. The latter is given approximately by[28] $\delta t = 4\rho/(3\gamma^3 c)$, and determines the spectral range emitted by each electron. The bunch length determines the spectral range over which the coherent enhancement occurs. For an electron energy of 10 MeV ($\gamma = 21$), and with $\rho = 1$ m, we obtain a δt of about 500 fs, which is comparable to the bunch length. The resulting spectral content extends up to about 1 THz, the same spectral range as for **a**. With all factors except γ the same, we see from equation (1) that the power radiated by a relativistic electron exceeds that from a conventional THz emitter by a factor of $\gamma^4 = 21^4 = 2 \times 10^5$.